Department of Pharmacology[1], Medical School of Ningbo University; Department of Health Management[2], Ningbo College of Health Sciences, Ningbo, Zhejiang, P.R. China

Fenofibrate reverses liver fibrosis in cholestatic mice induced by alpha-naphthylisothiocyanate

Zhuoheng Lu[1, #], Shengtao Li[1, #], Jia Luo[1], Yishuang Luo[1], Manyun Dai[1], Xiuting Zheng[1], Jiapeng Qiu[1], Julin Yang[2], Aiming Liu[1, *]

Received December 16, 2020, accepted January 15, 2021

**Corresponding author: Aiming Liu, Medical School of Ningbo University, Ningbo, Zhejiang 315211, China*
liuaiming@nbu.edu.cn
#These authors contributed equally to this work.

Pharmazie 76: 103-108 (2021) *doi: 10.1691/ph.2021.0988*

Cholestatic liver fibrosis occurs in liver injuries accompanied by inflammation, which develops into cirrhosis if not effectively treated in early stage. The aim of the study is to explore the effect of fenofibrate on liver fibrosis in chronic cholestatic mice. In this study, wild-type (WT) and Pparα-null (KO) mice were dosed alpha-naphthylisothiocyanate (ANIT) diet to induce chronic cholestasis. Induced liver fibrosis was determined by pathological biomarkers. Then fenofibrate 25 mg/kg was orally administrated to mice twice/day for 14 days. Serum and liver samples were collected for analysis of biochemistry and fibrosis. In WT mice, cholestatic biomarkers were increased by 5–8-fold and the expression of tissue inhibitors of metalloproteinases 1 (TIMP-1), Monocyte chemoattractant protein 1 (MCP-1), Collagen protein I (Collagen I) was increased by more than 10-fold. Fenofibrate significantly downgraded the biochemical and fibrotic biomarkers. In Western blot analysis, levels of collagen I and alpha-smooth muscle actin (α-SMA) were strongly inhibited by fenofibrate. In KO mice, liver fibrosis was induced successfully, but no improvement after fenofibrate treatment was observed. These data showed low-dose fenofibrate reverses cholestatic liver fibrosis in WT mice but not in KO mice, suggesting the dependence of therapeutic action on peroxisome proliferator-activated receptor alpha (PPARα). The study offers an additional therapeutic strategy for cholestatic liver fibrosis in practice.

1. Introduction

Chronic liver diseases are a major reason of morbidity and mortality, affecting 360 per 100,000 persons (Petitclerc et al. 2017). Liver fibrosis is featured by an excessive accumulation of extracellular matrix (ECM) including collagen which occurs in many chronic liver diseases. Patients with liver fibrosis are more susceptible to hepatitis C virus infection and the number of fibrotic patients is expected to rise over the next decades. Hepatic fibrosis is one of the risk factors triggering liver cirrhosis and carcinoma. And among the patients with hepatic carcinoma, 80-90% are suffering from chronic liver fibrosis (Chung et al. 2016). Liver fibrosis usually develops into cirrhosis, liver failure, portal hypertension lacking effective treatment (Bataller and Brenner 2005). In the late stage, many patients cannot survive without liver transplantation.

Cholestatic liver diseases are disorders of bile formation and/or flow, which often lead to cirrhosis and liver failure (Zakharia et al. 2018). Primary sclerosing cholangitis (PSC) and primary biliary cirrhosis (PBC) are two kinds of typical cholestasis (Boonstra et al. 2012, Invernizzi et al. 2017). PSC is strongly linked to inflammatory bowel diseases which are easy to develop colorectal and hepatobiliary malignancies (Claessen et al. 2009). The prevalence of PBC in southern China is 492 cases/million, and in Italy, about 279 per million (Griffiths et al. 2014; Marzioni et al. 2019). Additionally, cholestasis occurs in patients suffering from nonalcoholic fatty liver disease, where the incidence is over 40% in Asian countries (Sayiner et al. 2016). Adjacent adult hepatocytes are able to regenerate and to replace apoptotic and necrotic cells (Bataller and Brenner 2005). When the regeneration of injured hepatocytes fails, hepatocytes will be replaced by extracellular matrix proteins, alongside with inflammation. And the ECM components change from collagen IV, VI, and glycoproteins, proteoglycans to collagen I, III and fibronectin (Rojkind et al. 1979; Hahn et al. 1980; Brown et al. 2006).

Fenofibrate is an activator for transcription factor peroxisome proliferator-activated receptor alpha (PPARα). In the clinic, it is widely used in treating atherosclerosis-related hypertriglyceridemia and mixed hyperlipidemia (Fievet and Staels 2009; Grigorian et al. 2015; Cheung et al. 2016). For hepatic injury and apoptosis induced by bile duct ligation (BDL) in rats, short-term (6 weeks) administration of fenofibrate (100 mg/kg) reduced biochemical indicators and liver injury (Cindoruk et al. 2007). Fenofibrate also increased rat biliary phosphatidylcholine secretion to protect against liver injury (Ghonem et al. 2014). In PBC patients, treatment with ursodeoxycholic acid (UDCA) plus fenofibrate (200 mg/day) significantly improved serum ALP levels (Duan et al. 2018). For patients with asymptomatic PBC who responded incompletely to UDCA, the ALP level was partially decreased to (285±114.8 vs 186.9±76.2 IU/L) after fenofibrate treatment (100 mg/kg for patients under 60 kg and 150 mg/kg for patients above 60 kg) for 12 weeks (Dohmen et al. 2004). Thus, fenofibrate is beneficial for cholestasis in both animal models and human. However, its effect on cholestatic liver fibrosis is not clear.

In the present study, WT and KO mice were treated with a diet containing ANIT (0.05% in a commercial diet) to induce cholestatic liver fibrosis. Fenofibrate administration (25 mg/kg bid) for 2 weeks reversed the liver fibrosis in cholestatic mice. This action of fenofibrate suggests a new therapeutic approach for hepatic fibrosis in chronic liver diseases.

2. Investigations and results

2.1. Cholestasis and hepatic injury caused by ANIT

The relative gallbladder weight of group WT-A was increased by 3.4-fold in comparison with the WT-Ctrl group. It was decreased by 58.3% in the group WT-A-F. The relative gallbladder weight in group KO-A-D28 was increased by 6.6-fold compared to KO-Ctrl.

But in group KO-A-F, it was not modified by fenofibrate ($p<0.05$, Fig. 1A-B). In biomarkers analysis, the serum TBA was obviously increased by 4.7-, 3.0-, and 7.0-fold, respectively, on days 14, 21, and 28. ALP in group WT-A-D14 was increased by around 4-fold. During the following 14 days of ANIT administration, ALP maintained relatively stable. In group WT-A-F treated with fenofibrate on day 28, TBA and ALP were reduced by 58.7% and 44.3% respectively compared with WT-A group. In KO mice, TBA was increased by 6.2-, 4.3- and 4.8-fold on day 7, 14, 21 after ANIT challenge. Similarly, ALP was increased by 2.6-, 3.4- and 2.9-fold respectively. No attenuation of cholestasis was observed by fenofibrate treatment for either TBA or ALP ($p<0.05$, Fig. 1C-F).

In the chronic cholestasis, both AST and ALT in WT mice were increased by around 6.0-fold on day 14. Fenofibrate treatment for 14 days decreased AST and ALT by 61.0% and 44.4% in group WT-A-F. In KO mice, AST was increased by 2.3-, 3.2-, 3.8-fold and ALT was increased by 6.9-, 3.5-, 4.2-fold on day 7, 14, 21 after ANIT treatment. In contrast with those of WT mice, the tendency of biochemical indicators most kept the same level in group KO-A-F ($p<0.05$, Fig. 2A-D). These results showed that fenofibrate reduced chronic cholestatic liver injury with the dependence of PPARα.

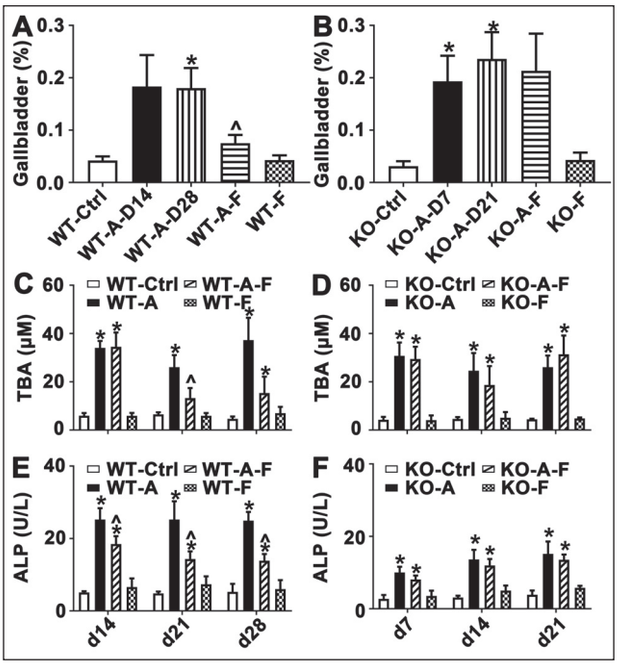

Fig. 1: Gallbladder change and biochemical analysis of cholestasis after ANIT and fenofibrate treatment. (A-B) Gallbladder change in the WT and KO mice respectively. (C-D) TBA in WT mice and KO mice. (E-F) ALP in the two types of mice. The data are expressed as mean±SD (n=5, *p<0.05, compared with WT-Ctrl/KO-Ctrl; ^p<0.05, compared with WT- A/KO- A). TBA, total bile acid; ALP, alkaline phosphatase.

2.2. *Inflammation and apoptosis in chronic cholestatic liver fibrosis*

In WT mice, the level of IL-1β mRNA was increased by 6.6-, 7.7-fold and IL-10 was increased by 3.0-, 4.2-fold on day 14 and 28 in the WT-A group. After fenofibrate treatment for 14 days, IL-1β and IL-10 were decreased by 77.4% and 62.4%, respectively. Similarly, their expression was also upregulated by 4.6-, 6.0-fold and 8.2-, 5.1-fold in KO mice on day 7 and 21. But it remained relatively stable during fenofibrate treatment ($p<0.05$, Fig. 3A-D). In analysis of apoptotic genes, Bcl2 and Bax were both increased by about 1-fold on day 14 and 4-fold on day 28 during ANIT challenge. In group WT-A-F, they were decreased by 61.3% and 73.6%, respectively. In KO mice, Bcl2 increased 5-8-fold and Bax were upregulated by 2-4-fold during ANIT challenge. Unlike WT mice, both genes were not decreased in group KO-A-F ($p<0.05$,

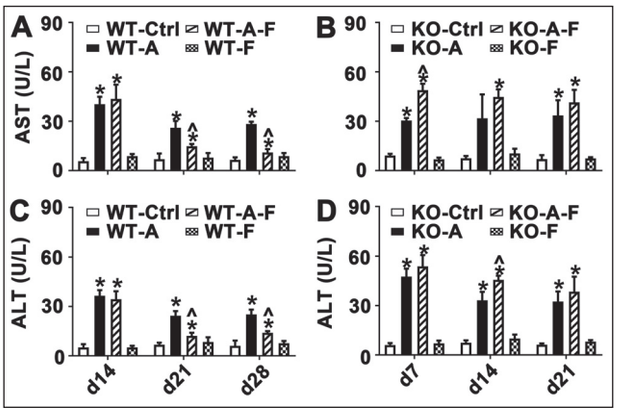

Fig. 2: Biochemical analysis of liver injury after ANIT and fenofibrate treatment. (A-B) AST change in the WT and KO mice respectively. (C-D) ALT in WT mice and KO mice. The data are expressed as mean±SD (n=5, *p<0.05, compared with WT-Ctrl/KO-Ctrl; ^p<0.05, compared with WT- A/KO- A). AST, aspartate aminotransferase; ALT, alanine aminotransferase.

Fig. 3E-H). These data suggested that inflammation and apoptosis, which accompanied chronic cholestasis, were inhibited by fenofibrate.

2.3. *Chronic cholestatic liver fibrosis and the action of fenofibrate*

In pathological analysis of the liver tissues in WT-Ctrl and KO-Ctrl mice, the histological observation was quite abnormal. In mice challenged with ANIT for 14 days, large collagen fibers were

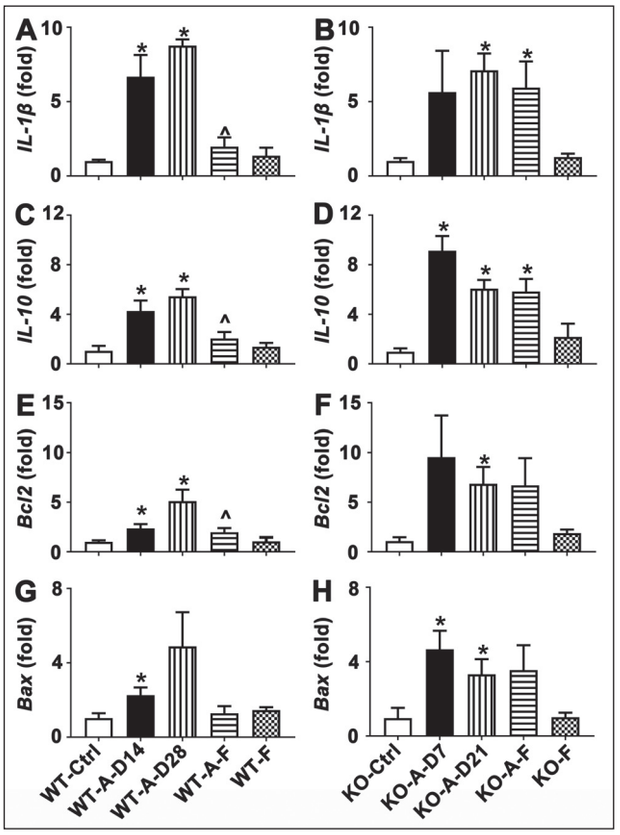

Fig. 3: Gene expression changes of inflammation and apoptosis factors in liver tissues. (A-B) IL-1β mRNA level in WT and KO mice respectively. (C-D) IL-10 mRNA level in WT and KO mice respectively. (E-F) Bcl2 mRNA level in WT and KO mice respectively. (G-H) Bax mRNA level in WT and KO mice respectively. The mRNA levels were measured by quantitative PCR and normalized by 18S rRNA. The results expressed as mean±SD (n=5, *p<0.05, compared with WT-Ctrl/KO-Ctrl; ^p<0.05, compared with WT- A-D28/KO-A-D21). IL-1β, Interleukin-1β; IL-10, Interleukin-10; Bcl2, B-cell lymphoma-2; Bax, BCL2 associated X, apoptosis regulator.

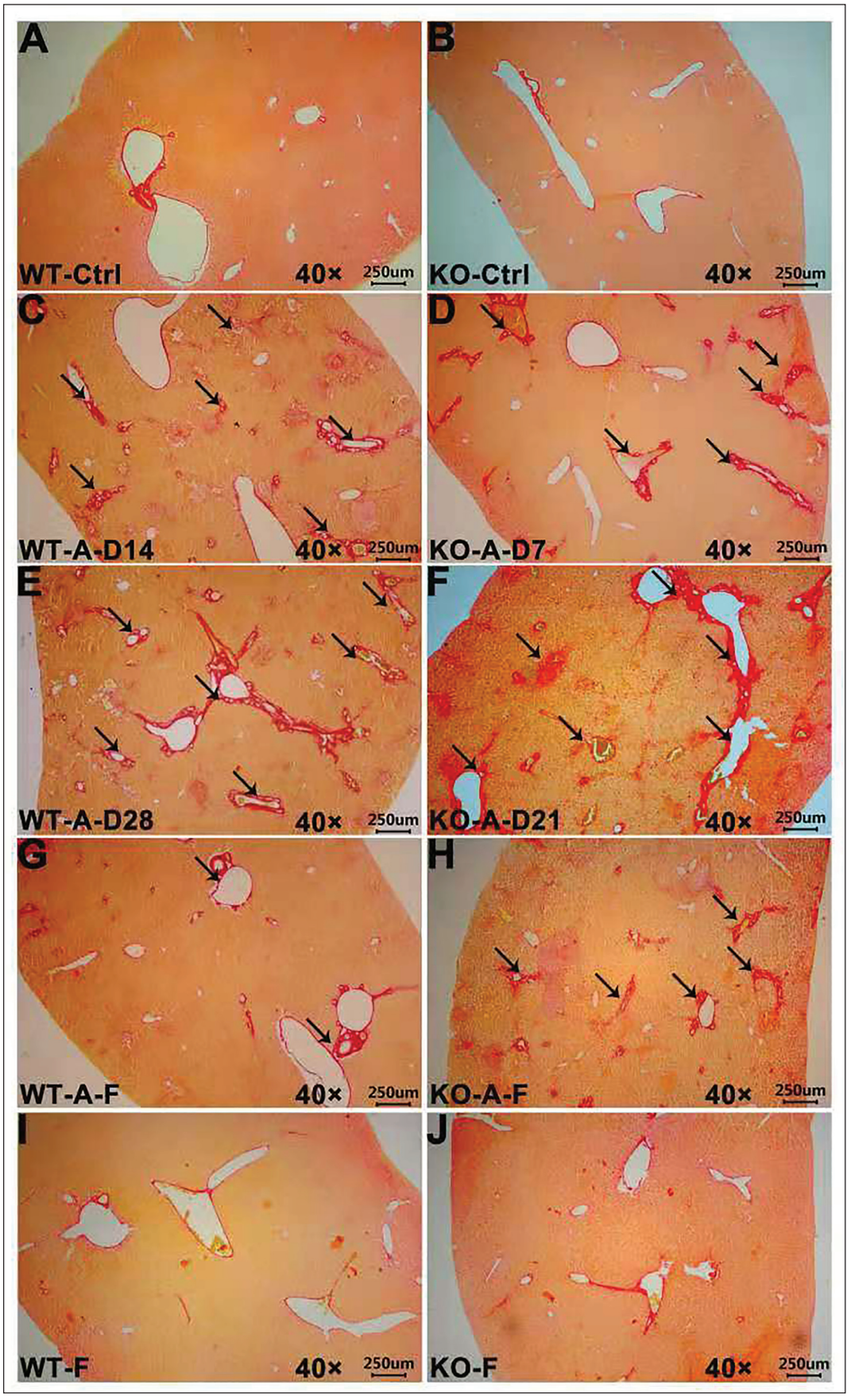

Fig. 4: Histopathological analysis of liver tissues indicating the hepatic fibrosis and the reverse effect of fenofibrate. (A-B) Sirius Red staining of liver tissues in the WT-Ctrl and KO-Ctrl groups (40X). (C-D) Sirius Red staining of liver tissues in the WT-A-D14 and KO-A-D7 groups (40X). (E-F) Sirius Red staining of liver tissues in the WT-A-D28 and KO-A-D21 groups (40X). (G-H) Sirius Red staining of liver tissues in the WT-A-F and KO-A-F groups (40X). (I-J) Sirius Red staining of liver tissues in the WT-F and KO-F groups (40X).

observed, indicating the occurrence of hepatic fibrosis, but it was not different between the two mouse lines. In WT-A-F group, an evident reduction of collagen fibers was observed compared with those in WT-A group. In contrast, in KO-A-F group, no decreasing tendency was observed (Fig. 4A-H). Thus, the above observations showing cholestatic fibrosis were inhibited by fenofibrate in dependence of PPARα.

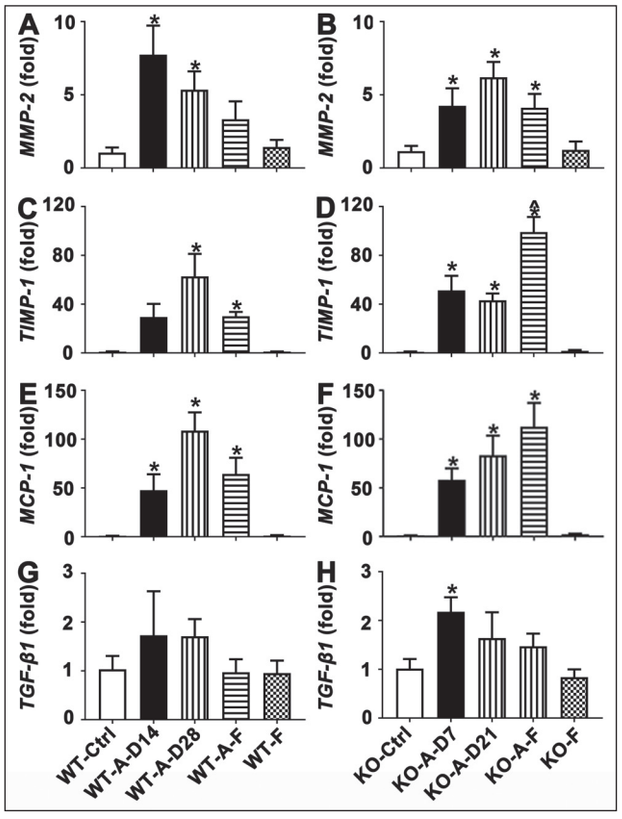

Fig. 5: Gene expression levels of liver fibrosis and the role of fenofibrate in liver tissues. (A-B) MMP-2 mRNA level in WT and KO mice respectively. (C-D) TIMP-1 mRNA level in WT and KO mice respectively. (E-F) MCP-1 mRNA level in WT and KO mice respectively. (G-H) TGF-β1 mRNA level in WT and KO mice respectively. The mRNA levels were measured by quantitative PCR and normalized by 18S rRNA. The results expressed as mean±SD (n=5, *p<0.05, compared with WT-Ctrl/KO-Ctrl; ^p<0.05, compared with WT- A-D28/KO- A-D21). MMP-2, matrix metalloproteinases 2; TIMP-1, tissue inhibitors of metalloproteinases 1; MCP-1, monocyte chemoattractant protein 1; TGF-β1, transforming growth factor-β 1.

In the transcription analysis of the fibrotic factors, MMP-2 was increased by 4-6-fold and TIMP-1 was increased by 30-60-fold on day 14, 28 respectively in group WT-A. MCP-1 mRNA level was upregulated by 47-fold and 107-fold in WT mice after ANIT treatment for 14 and 28 days. TGF-β1 mRNA level was only slightly elevated on day 28 in WT mice. The transcription of collagen I increased by 13- and 6-fold on day 14 and 28 in group WT-A. 37.7%, 52.0%, 40.7% and 40.4% reduction of MMP-2, TIMP-1, MCP-1 and Collagen I expression were observed in group WT-A-F ($p<0.05$, Fig. 5A, C, E and G; Fig. 6A and C).

In KO mice, there was a 3-5-fold increase of MMP-2 expression. And TIMP-1 was increased to 45-55-fold after ANIT treatment for 7 and 21 days. For MCP-1, the increase was increased by about 55-85-fold in comparison with that of the normal control group on day 7 and 21. TGF-β1 mRNA was only increased by 1-fold on the day of ANIT treatment 7 days. The collagen I and α-SMA mRNA level were upregulated by around 13–15-fold and 2–3-fold compared with those in group KO-A. Contrary to WT mice, fenofibrate resulted to an increase of TIMP-1 and MCP-1, even the expression of TIMP-1 was by more than 1-fold in group KO-A-F compared with group KO-A-D21. And the level of collagen I expression did not show any change in group KO-A-F ($p<0.05$, Fig. 5B, D, F and H; Fig. 6B and D). This result may be due to the absence of PPARα, which leads to the failure of fenofibrate to provide protection, and thus the degree of hepatic fibrosis increases rather than decreases.

In western-blot, ANIT challenge activated COL1A1 and α-SMA in WT mice. The protein COL1A1 was obviously inhibited in WT mice treated with fenofibrate. Although the change of α-SMA protein expression was not as significant as that of COL1A1, the expression of α-SMA was also inhibited after fenofibrate treatment and was similar to control. For the KO mice, the proteins were increased in group KO-A-D21 but not modified in group KO-A-D7 group. And the expression of protein α-SMA in group KO-A-F was a little bit higher than those in mice treated only with ANIT conversely. In addition, WT-F and KO-F groups were same as the control, no significant difference between these groups (Fig. 6E-F).

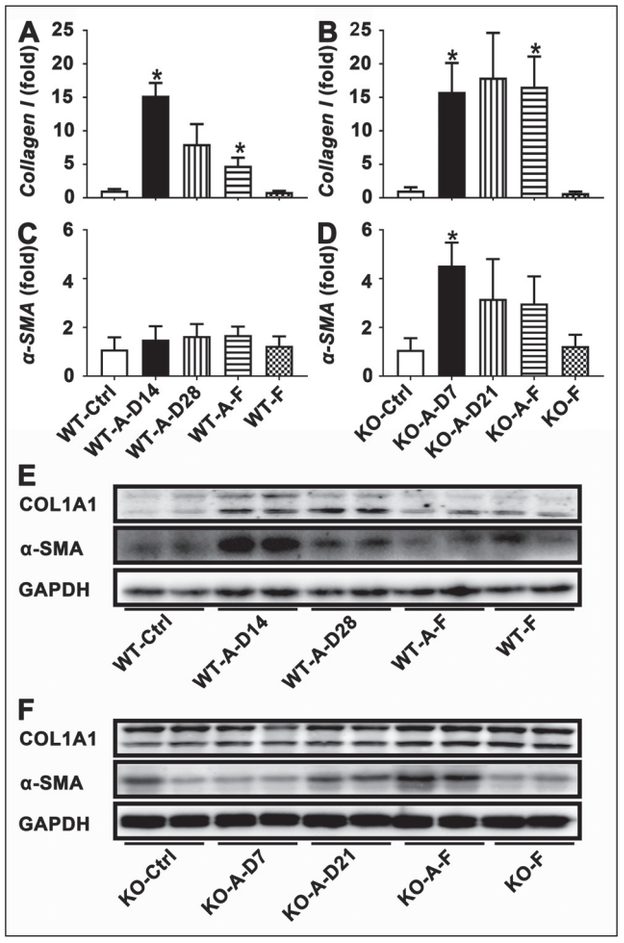

Fig. 6: Analysis of the degree of liver fibrosis and effects of fenofibrate at mRNA and protein level. (A-B) Collagen I mRNA level in WT and KO mice respectively. (C-D) α-SMA mRNA level in WT and KO mice respectively. The mRNA levels were measured by quantitative PCR and normalized by 18S rRNA. (E-F) Western blot analysis of the role of fenofibrate mediated by PPARα. GAPDH was used as a loading control. The results expressed as mean±SD (n=5, *p<0.05, compared with WT-Ctrl/KO-Ctrl; ^p<0.05, compared with WT- A-D28/KO- A-D21). Collagen I, collagen protein I; α-SMA, alpha-smooth muscle actin; GAPDH, glyceraldehyde-3-phosphate dehydrogenase.

3. Discussion

Cholestasis can be induced by ANIT, bile duct ligation (BDL) and carbon tetrachloride (CCl_4). The liver fibrosis induced by BDL and CCl_4 had the characteristics of simplicity and typical

pathological changes. However, BDL would easily cause mechanical damage to organs through surgery, while CCl_4 a high mortality rate, and excessive dose may lead to the early formation of cirrhosis. The cholestasis induced by ANIT was the closest to intrahepatic cholestasis in human in pathological and physiological reactions (Tjandra et al. 2000). All the above three methods in the acute cholestasis models are widely used. However, chronic cholestasis is the real scenario which occurs mostly in clinical practice. Therefore, this experiment tried to use ANIT to build a chronic model. In the present study, after only 2 weeks of modeling in WT mice, the markers of cholestasis and liver fibrosis were significantly upregulated. And the pathology clearly showed a large amount of collagen deposition, indicating that the mice were successfully induced to produce cholestatic liver fibrosis.

In this study, although both mice lines were induced to develop cholestatic liver fibrosis, it took twice time in WT mice than that in KO mice. In a 48-hour acute experiment involving ANIT-induced cholestasis, serum biochemical parameters, histopathology and expression of inflammatory factors all showed a lower liver injury and inflammation level in WT mice (Dai et al. 2018). Similarly, the time difference between two mice lines in this experiment also indicted a protective role of basal PPARα. This result accorded with above data in the acute model. Therefore, the longitudinal difference of cholestasis induction between the two mice lines was supposed to be associated with the anti-inflammation of basal PPARα.

In chemotaxis, neutrophils and macrophages move to the liver, causing an inflammatory response. They also produce cytokines, which drive hepatic satellite cells to transform to be myofibroblasts expressing α-*SMA* (Xu et al. 2012). TGF-β1, is an important fibrogenic cytokine, inducing HSCs to produce autocrine and paracrine, then promotes abnormal proliferation and excessive deposition of ECM, leading to fibrosis (Galicia-Moreno et al. 2013; Khedr and Khedr 2017). TGF-β1 inhibited ECM degradation and thus stimulated the increase of TIMPs (Casas-Grajales et al. 2017). In this study, the changes of *MMP-2*, *TIMP-1*, *MCP-1* and *Collagen I* mRNA were increased by 5-, 30-, 50-, and 10-fold in WT mice challenged with ANIT. Protein levels of collagen I and α-SMA were also upregulated after ANIT challenge. The inconsistency between the protein level and the corresponding mRNA expression level may be caused by the regulation of different chemical molecular modification after the mRNA transcription translation, thus presenting the final protein level different from the mRNA expression level. This research group did not carry out corresponding research in this aspect, but this may provide a new idea for the follow-up experimental direction. The modification tendency of the above indicators demonstrated the cholestatic liver fibrosis was induced by 14-day ANIT treatment in WT mice.

In clinical reports, fenofibrate (150-200 mg/kg/day) improved liver biochemical responses in PBC patients who partially respond to UDCA (Han et al. 2012; Hegade et al. 2016). Fenofibrate (50-200 mg/kg/day) regulated the synthesis and metabolism of bile acids and was preventive in intrahepatic cholestasis induced by BDL or drugs in rodent models (Cindoruk et al. 2007; Shi et al. 2010; El-Sisi et al. 2013). A recent study indicated that low-dose fenofibrate (25 mg/kg, twice daily) also prevented cholestatic liver injury in an acute cholestasis model (Dai et al. 2017). In this study, the same dose level reversed cholestatic liver fibrosis in WT mice, but not the KO mice. Considering that fenofibrate causes liver injury and acute cholestatic hepatitis in some cases (Fartoux-Heymann et al. 2001; Ho et al. 2004), this action of low-dose fenofibrate (1/4 of anti-dyslipidemia level) offers a new therapeutic strategy for cholestatic liver fibrosis with much lower toxicity risk.

To sum up, 14-day ANIT administration could induce chronic cholestatic liver fibrosis in WT mice. Basal PPARα was protective against the development of cholestatic liver fibrosis. More importantly, low-dose fenofibrate (25 mg/kg, bid) significantly reversed cholestatic liver fibrosis suggesting an exciting therapeutic approach for liver fibrosis.

4. Experimental

4.1. Chemicals and reagents

Kits for the hepatic injury biomarker aspartate aminotransferase (AST) and alanine aminotransferase (ALT), and those for cholestasis biomarkers alkaline phosphatase (ALP), total bile acid (TBA), were acquired from Meikang Biotechnology (Ningbo, China). Fenofibrate and alpha-naphthylisothiocyanate (ANIT) were bought from Sigma-Aldrich (St Louis, MO). Sirius Red staining solution was bought from Shanghai Source Leaf Biotechnology Co., Ltd (Shanghai, China). Antibody against Collagen I (1:1000, #46888) were gotten from Signalway Antibody (SAB, USA) and antibodies against α-SMA (1:5000, ab5694) and GAPDH (1:5000, ab181602) were bought from Abcam (MA, USA). PMSF was bought from Solarbio (Shanghai, China) and BCA kit for protein quantification was product by CWBIO (Beijing, China). TRIzol was purchased from Omega Bio-Tek (Guangzhou, China). The kit for reverse transcription and UltraSYBR Mixture were purchased from CWBIO (Beijing, China). Pure water was prepared by Milli-Q50 SP Water System (Hangzhou, China).

4.2. Animals and treatments

The Ppara-null (KO) mice were described in earlier studies (PMID: 753910) and were on the 129/Sv genetic background as were the WT control mice. All procedures were performed in compliance with relevant laws and institutional guidelines of Ningbo University and the appropriate institutional committees have approved them. All animals received humane care and were treated in accordance with the Institute of Laboratory Animal Resource guidelines. Before the experiment, 23±2 g male mice were adaptively reared for 7 days at the Animal Center of Ningbo University College. The housing environment was kept under a temperature of 24±1 °C, a humidity of 50-60% and a normal 12-hour light-dark cycle.

The WT and KO mice were randomly assigned to 4 groups: vehicle/control (WT-Ctrl, KO-Ctrl, n=5), ANIT/control (WT-A, KO-A, n=10), ANIT/fenofibrate (WT-A-F, KO-A-F, n=5), fenofibrate/control (WT-F, KO-F, n=5). The WT-Ctrl and KO-Ctrl groups were treated with commercial diets throughout the experiment. The WT group WT-A, WT-A-F, and KO group KO-A, KO-A-F were dosed the ANIT diet (the dose level was around 75 mg/kg). Five of the mice in groups WT-A and KO-A were sacrificed on the morning of day 14 and day 7 (designated as WT-A-D14 and KO-A-D7), to determine the induction of cholestasis. The other 5 mice in the above two groups were sacrificed when the experiment was finished on day 28 and 21, which were designated as WT-A-D28, KO-A-D21 respectively.

The mice in group WT-A-F and KO-A-F were treated with the diet containing ANIT and fenofibrate was used by intragastric administration twice a day from day 15 and day 8 respectively. The groups WT-F and KO-F were treated with fenofibrate (25 mg/kg) twice a day by intragastric administration as the above.

Tail bleeding was performed every 3 days in group WT-A and KO-A to monitor biochemical modification during chronic ANIT treatment. When the mice were sacrificed, blood was collected for biochemical analysis. A portion of fresh liver tissue was excised and washed with phosphate buffered saline, and then fixed in a 10% neutral formalin fixative. The remaining liver tissues were immediately frozen in dry ice and placed in a -80 °C refrigerator for QPCR and protein analysis.

4.3. Biochemical analysis

The serum TBA, ALP, AST and ALT were determined by a validated rate method using the Multiskan GO (Thermo, USA). The procedures were performed according to the descriptions in the kits.

4.4. Histopathology analysis

The liver tissues fixed in formalin buffer were cut into blocks of 3-5 mm. Then they were subjected to gradient dehydration, de-alcoholization, transparency, and embedding. Sections (4 μm) were cut from paraffin block, which were then subjected to Sirius red staining. Finally, the sections were observed using microscope (Carl Zeiss, Axiostar plus).

4.5. Transcription analysis

Frozen liver tissues were fully lysed in TRIzol and then homogenized using MagNALyser (Roche, USA). The concentration of RNA was measured by Multiskan Go (Thermo Scientific, Waltham, USA) after centrifugation, precipitation, washing, and dissolution. The purity of RNA was higher at OD260/OD280=1.8-2.0. Reverse transcription with the reverse transcription kit was done as previously described (Tan et al. 2016). The primer sequences, listed in the Table, were extracted from https://pga.mgh.harvard.edu/primerbank/. Quantitative polymerase chain reaction (Q-PCR) amplification on 384-well plates was performed in a 5 μL system containing 1 μL cDNA, 2.2 μL UltraSYBR Mixture, 0.1μL primer and 1.6 μL double distilled water using LightCycler 480 II (Roche, USA).

4.6. Immuno-blot assay

The frozen liver samples were fully lysed in RIPA with 1% PMSF and then homogenized adequately. After protein quantification, the samples were centrifuged at 13000 rpm for 20 min to collect the supernatant at 4 °C. An equal volume of 5X SDS-PAGE loading buffer was mixed with the protein, and then boiling for 8 min was performed. The blots were transferred to PVDF membranes after separation using 10% SDS-polyacrylamide gels. Subsequently, 5% milk was used for 3.5-hour blocking. The membranes were incubated with primary antibody at 4 °C overnight. After washing with phosphate buffer, it was incubated with a secondary antibody for

Table: The primers used for the Q-PCR assessment in this study

Genes names	Forward primer	Reverse primer	Size (bp)
IL-1β	TGTGAAATGCCACCTTTTGA	GGTCAAAGGTTTGGAAGCAG	94
IL-10	TGTCAAATTCATTCATGGCCT	ATCGATTTCTCCCCTGTGAA	108
Bcl2	GGTCTTCAGAGACAGCCAGG	GATCCAGGATAACGGAGGCT	94
Bax	GATCAGCTCGGGCACTTTAG	TTGCTGATGGCAACTTCAAC	100
MMP-2	TGCTGGGTAGAGTCTAGGGT	TGTTTGCAGATCTCCGGAGT	140
TIMP-1	GAGACACACCAGAGCAGATACC	CCAGGTCCGAGTTGCAGAAG	146
MCP-1	GCTTCTGGGCCTGTTGTTC	CTGCTGCTGGTGATTCTCTTGT	156
TGF-β1	GTGTGGAGCAACATGTGGAACTCTA	TTGGTTCAGCCACTGCCGTA	143
Collagen I	CCTGGCAAAGACGGACTCAAC	GCTGAAGTCATAACCGCCACTG	150
α-SMA	GGCTCTGGGCTCTGTAAGG	CTCTTGCTCTGGGCTTCATC	148
18S rRNA	ATTGGAGCTGGAATTACCGC	CGGCTACCACATCCAAGGAA	102

2 h at room temperature. ECL substrates were added to the blotted PFDV and the images were recorded by chemical imaging illumination system (Shanghai, China).

4.7. Statistical analysis

The data were expressed as the mean±SD. Data analysis was performed using SPSS 17 for Windows. One-way ANOVA, followed by Dunnett's *post hoc* comparisons was carried out for difference examination. The responses in ANIT/ANIT-Feno/Feno and Control groups, ANIT-D28 and ANIT-Feno in two mice lines were compared using Student's t-test. The analyzed data was plotted by GraphPad Prism 7. Significance was considered different when p values were below 0.05, which was marked with asterisks or cusp triangle in the graphs.

Funding: This study was supported by the Ningbo Welfare Technology Program (202002N3160), Zhejiang Public Welfare Technology Research Program (LGD19H070001, LY20H030001) and the K. C. Wong Magna Fund in Ningbo University.

Conflicts of interest: The authors declare that they have no conflicts of interest related to this article.

References

Bataller R, Brenner DA (2005) Liver fibrosis. J Clin Invest 115: 209–218.

Boonstra K, Beuers U, Ponsioen CY (2012) Epidemiology of primary sclerosing cholangitis and primary biliary cirrhosis: a systematic review. J Hepatol 56: 1181–1188.

Brown B, Lindberg K, Reing J, Stolz DB, Badylak SF (2006) The basement membrane component of biologic scaffolds derived from extracellular matrix. Tissue Eng 12: 519–526.

Casas-Grajales S, Vazquez-Flores LF, Ramos-Tovar E, Hernandez-Aquino E, Flores-Beltran RE, Cerda-Garcia-Rojas CM, Camacho J, Shibayama M, Tsutsumi V, Muriel P (2017) Quercetin reverses experimental cirrhosis by immunomodulation of the proinflammatory and profibrotic processes. Fundam Clin Pharmacol 31: 610–624.

Cheung AC, Lapointe-Shaw L, Kowgier M, Meza-Cardona J, Hirschfield GM, Janssen HL, Feld JJ (2016) Combined ursodeoxycholic acid (UDCA) and fenofibrate in primary biliary cholangitis patients with incomplete UDCA response may improve outcomes. Aliment Pharmacol Ther 43: 283–293.

Chung SI, Moon H, Ju HL, Cho KJ, Kim DY, Han KH, Eun JW, Nam SW, Ribback S, Dombrowski F, Calvisi DF, Ro SW (2016) Hepatic expression of Sonic Hedgehog induces liver fibrosis and promotes hepatocarcinogenesis in a transgenic mouse model. J Hepatol 64: 618–627.

Cindoruk M, Kerem M, Karakan T, Salman B, Akin O, Alper M, Erdem O, Unal S (2007) Peroxisome proliferators-activated alpha agonist treatment ameliorates hepatic damage in rats with obstructive jaundice: an experimental study. BMC Gastroenterol 7: 44.

Claessen MM, Vleggaar FP, Tytgat KM, Siersema PD, van Buuren HR (2009) High lifetime risk of cancer in primary sclerosing cholangitis. J Hepatol 50: 158–164.

Dai M, Hua H, Lin H, Xu G, Hu X, Li F, Gonzalez FJ, Liu A, Yang J (2018) Targeted metabolomics reveals a protective role for basal PPARalpha in cholestasis induced by alpha-naphthylisothiocyanate. J Proteome Res 17: 1500–1508.

Dai M, Yang J, Xie M, Lin J, Luo M, Hua H, Xu G, Lin H, Song D, Cheng Y, Guo B, Zhao J, Gonzalez FJ, Liu A (2017) Inhibition of JNK signalling mediates PPARalpha-dependent protection against intrahepatic cholestasis by fenofibrate. Br J Pharmacol 174: 3000–3017.

Dohmen K, Mizuta T, Nakamuta M, Shimohashi N, Ishibashi H, Yamamoto K (2004) Fenofibrate for patients with asymptomatic primary biliary cirrhosis. World J Gastroenterol 10: 894–898.

Duan W, Ou X, Wang X, Wang Y, Zhao X, Wang Q, Wu X, Zhang W, Ma H, You H, Jia J (2018) Efficacy and safety of fenofibrate add-on therapy for patients with primary biliary cholangitis and a suboptimal response to UDCA. Rev Esp Enferm Dig 110: 557–563.

El-Sisi A, Hegazy S, El-Khateeb E (2013) Effects of three different fibrates on intrahepatic cholestasis experimentally induced in rats. PPAR Res 2013: 781348.

Fartoux-Heymann L, Narcy-Lambare B, Labayle D, Fischer D (2001) [Acute hepatitis and drug dermatitis due to fenofibrate (Secalip)]. Ann Med Interne (Paris) 152: 353–354.

Fievet C, Staels B (2009) Combination therapy of statins and fibrates in the management of cardiovascular risk. Curr Opin Lipidol 20: 505–511.

Galicia-Moreno M, Favari L, Muriel P (2013) Trolox mitigates fibrosis in a bile duct ligation model. Fundam Clin Pharmacol 27: 308–318.

Ghonem NS, Ananthanarayanan M, Soroka CJ, Boyer JL (2014) Peroxisome proliferator-activated receptor alpha activates human multidrug resistance transporter 3/ATP-binding cassette protein subfamily B4 transcription and increases rat biliary phosphatidylcholine secretion. Hepatology 59: 1030–1042.

Griffiths L, Dyson JK, Jones DE (2014) The new epidemiology of primary biliary cirrhosis. Semin Liver Dis 34: 318–328.

Grigorian AY, Mardini HE, Corpechot C, Poupon R, Levy C (2015) Fenofibrate is effective adjunctive therapy in the treatment of primary biliary cirrhosis: A meta-analysis. Clin Res Hepatol Gastroenterol 39: 296–306.

Hahn E, Wick G, Pencev D, Timpl R (1980) Distribution of basement membrane proteins in normal and fibrotic human liver: collagen type IV, laminin, and fibronectin. Gut 21: 63–71.

Han XF, Wang QX, Liu Y, You ZR, Bian ZL, Qiu DK, Ma X (2012) Efficacy of fenofibrate in Chinese patients with primary biliary cirrhosis partially responding to ursodeoxycholic acid therapy. J Dig Dis 13: 219–224.

Hegade VS, Khanna A, Walker LJ, Wong LL, Dyson JK, Jones DEJ (2016) Long-term fenofibrate treatment in primary biliary cholangitis improves biochemistry but not the UK-PBC risk score. Dig Dis Sci 61: 3037–3044.

Ho CY, Kuo TH, Chen TS, Tsay SH, Chang FY, Lee SD (2004) Fenofibrate-induced acute cholestatic hepatitis. J Chin Med Assoc 67: 245–247.

Invernizzi P, Floreani A, Carbone M, Marzioni M, Craxi A, Muratori L, Vespasiani Gentilucci U, Gardini I, Gasbarrini A, Kruger P, Mennini FS, Ronco V, Lanati E, Canonico PL, Alvaro D (2017) Primary Biliary Cholangitis: advances in management and treatment of the disease. Dig Liver Dis 49: 841–846.

Khedr NF, Khedr EG (2017) Branched chain amino acids supplementation modulates TGF-beta1/Smad signaling pathway and interleukins in CCl4 -induced liver fibrosis. Fundam Clin Pharmacol 31: 534–545.

Marzioni M, Bassanelli C, Ripellino C, Urbinati D, Alvaro D (2019) Epidemiology of primary biliary cholangitis in Italy: Evidence from a real-world database. Dig Liver Dis 51: 724–729.

Petitclerc L, Sebastiani G, Gilbert G, Cloutier G, Tang A (2017) Liver fibrosis: Review of current imaging and MRI quantification techniques. J Magn Reson Imaging 45: 1276–1295.

Rojkind M, Giambrone MA, Biempica L (1979) Collagen types in normal and cirrhotic liver. Gastroenterology 76: 710–719.

Sayiner M, Koenig A, Henry L, Younossi ZM (2016) Epidemiology of nonalcoholic fatty liver disease and nonalcoholic steatohepatitis in the United States and the Rest of the World. Clin Liver Dis 20: 205–214.

Shi QY, Lin YG, Zhou X, Lin YQ, Yan S (2010) [Expression of FXR mRNA, PPAR alpha mRNA and bile acid metabolism related genes in intrahepatic cholestasis of pregnant rats]. Zhonghua Gan Zang Bing Za Zhi 18: 927–930.

Tan Z, Liu A, Luo M, Yin X, Song D, Dai M, Li P, Chu Z, Zou Z, Ma M, Guo B, Chen B (2016) Geniposide inhibits alpha-naphthylisothiocyanate-induced intrahepatic cholestasis: the downregulation of STAT3 and NFκB signaling plays an important role. Am J Chin Med 44: 721–736.

Tjandra K, Sharkey KA, Swain MG (2000) Progressive development of a Th1-type hepatic cytokine profile in rats with experimental cholangitis. Hepatology 31: 280–290.

Xu R, Zhang Z, Wang FS (2012) Liver fibrosis: mechanisms of immune-mediated liver injury. Cell Mol Immunol 9: 296–301.

Zakharia K, Tabibian A, Lindor KD, Tabibian JH (2018) Complications, symptoms, quality of life and pregnancy in cholestatic liver disease. Liver Int 38: 399–411.